TECNICA ITALIANA-Italian Journal of Engineering Science
Vol. 65, No. 2-4, July, 2021, pp. 391-400
Journal homepage: http://iieta.org/journals/ti-ijes

Toward the First Italian Elastocaloric Device: Projecting and Developing Steps

Luca Cirillo[1*], Adriana Rosaria Farina[1], Adriana Greco[1], Claudia Masselli[1], Federico Scarpa[2], Luca Antonio Tagliafico[2]

[1] Department of Industrial Engineering DII, University of Naples "Federico II", P.le Tecchio 80, Naples 80125, Italy
[2] Department of Mechanical, Energy, Management and Transportation Engineering DIME, University of Genoa, via alla Opera Pia 15, Genoa 16100, Italy

Corresponding Author Email: luca.cirillo2@unina.it

https://doi.org/10.18280/ti-ijes.652-437

Received: 10 March 2021
Accepted: 26 May 2021

Keywords:
refrigeration, elasto-caloric, shape-memory-alloy, prototype, sustainable, cooling

ABSTRACT

Nowadays about 20% of the worldwide energy consumption is attributable to refrigeration that is almost entirely based on vapor compression refrigeration. The elastocaloric refrigeration is being considered in the recent years as one of the most promising alternatives to vapour compression cooling technology.
It is based on the latent heat associated with the transformation process of the martensitic phase, found in Shape Memory Alloys (SMA) when they are subjected to uniaxial stress cycles of loading and unloading. SMAs are characterized by the mechanical property of being able to return to the initial form once the uniaxial stress has been removed. Currently the prototypes of elastocaloric cooler developed in the world are less than ten units and they are not close to the industrialization and commercialization, yet.
This contribution presents the design processes and the steps of development of the first Italian elastocaloric device: SSUSTAIN-EL. This research involves part of a bigger Italian project, called SUSSTAINEBLE, that involves three research institutes: University of Naples Federico II, University of Genoa and the National Research Council. The aim of research group is the developing of a demonstrative prototype of a continuously elastocaloric cooler, which can represent a fundamental step as "proof of concept".

1. INTRODUCTION

Refrigeration and air conditioning are arguably two of the most significant innovations of the 20th century that have transformed society everywhere by improving health, hygiene, and the overall quality of life. In recent years, refrigeration technology has become far more advanced than the Freon-powered clunkers of the 1960s. Businesses can significantly increase their energy efficiency and sustainability by implementing new technologies for managing, maintaining, and retiring refrigeration systems [1, 2]. The Montreal Protocol [3] set regulations for the production and consumption of these substances in the 1990s: CFCs were phased out in developed countries in 1996, be followed by HCFCs (phased out within 2020) and HFCs (beginning in 2015 and reduced by 85% within 2036) [4-8]. To date, HFCs are still the most manufactured and distributed type of refrigerants. Direct emissions of ODS (Ozone-Depleting Substances) typically occur during refrigeration system maintenance or disposal when the ozone-depleting gases trapped in the insulating foam and refrigerant charge of the machine escape into the atmosphere. However, it is equally problematic when refrigerant leaks occur during regular operation.

It is a crucial point to focus on innovative sustainable refrigeration techniques in place of vapour compression-based systems. Solid-state cooling technologies have gained great interest in recent years [9] and represent a new valid alternative to vapour compression cooling systems [10]. It has been demonstrated that solid-state refrigerators have an energy efficiency of more than 50% of the typical vapour-compression refrigerators. Solid-state cooling systems have no moving parts. For this reason, they offer high reliability and low maintenance compared to other types of cooling or heating equipment. Solid-state cooling systems offer low noise performance and are ideal for medical offices, laboratories, and all other places where noise reduction is a factor. Solid-state cooling systems are ecologically clean since no CFC, HCFC, or even HFC types of refrigerants are involved in the process. The core of the solid-state systems is the caloric effect: a physical phenomenon of several solid-state materials. Solid-state caloric systems rely on a reversible thermal phenomenon to provide cooling (or heating) when a magnetic [11] or electric field, pressure [12] or uniaxial stress varies.

Elastocaloric materials can cause significant temperature variations if subjected to a mechanical loading/unloading cycles without using high energy to activate a magnetic or electric field which instead must be activated for all other caloric material [13]. The elastocaloric cooling effect is visible using Shape Memory Alloy (SMA). As shown in Figure 1, the shape-memory effect or superelasticity of a SMA depends on its temperature: above austenite stability temperature (Af), a SMA is superplastic and below martensite stability temperature (Mf), exhibits shape-memory behaviour. These temperatures depend on the uniaxial stress applied. This makes SMAs very interesting to apply in various sectors such as automotive, robotics, civil engineering, biomedical (orthodontic wires, for example) [14]. Using this properties of

the SMA two kind of cycle are possible: the thermal driven cycle (characteristics of a heat engine) and the stress driven cycle (used for a cooling or heating pump system). In the stress driven cycle, the SMA is initially fully austenite under the stress-free state at the application temperature. During the loading phase, when the stress on the SMA exceeds the "saturation stress" of phase change, the austenite starts to transform into the martensite phase releasing latent heat to the ambient, reducing entropy. The reverse-phase change, from martensite to austenite, occurs during unloading. However, the hysteresis phenomenon does not permit that the saturation stress of unloading is equal to that of loading, as reported in the work of Michaelis et al. [15]. In this phase, the entropy increases and the latent heat is absorbed from the SMA material producing the typical cooling effect, as shown in Figure 2.

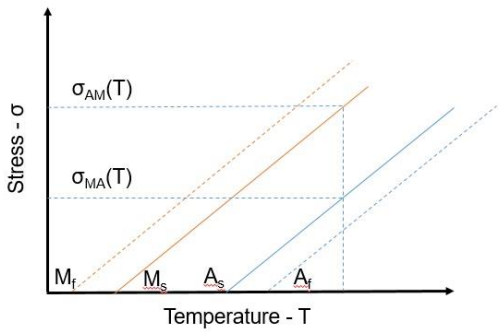

Figure 1. Diagram stress vs temperature

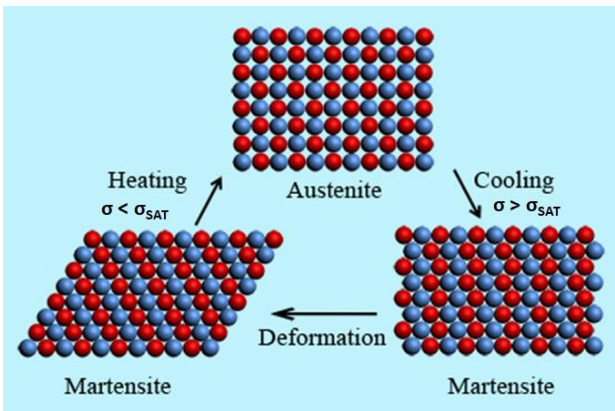

Figure 2. The transformation from austenite to martensite phase - cooling effect

It is possible to consider all SMAs materials as elastocaloric materials when they undergo a stress-induced transformation. Their transformation temperatures should be below the operating temperature for the desired application.

To develop an air conditioning system is necessary to produce the elastocaloric effect inside a cooling cycle to remove heat from the ambient. In a Brayton-based cycle the caloric materials operate both as refrigerant and as regenerator. Active regenerator cycles have long been used in magnetocaloric cooling. The adiabatic temperature variations with the active material's magnetization allow multiple materials with Curie temperatures calibrated in the operating conditions to be used [16]. It has proposed a regenerative cycle in the work of Aprea et al. [17] to allow the device (in their case, heat pump) to operate at temperature spans higher than the adiabatic temperature change of the material. They have provided an overview of the result collected by employing a broad set of different-effects caloric materials, including barocaloric ones. A regenerative cycle for elastocaloric systems is therefore a good opportunity.

The common magnetocaloric material used in many research projects is the Gadolinio (rare earth material), and currently, only 75 magnetocaloric prototypes are close to commercialization on a large scale. Many theoretical works define energy savings as around 50% compared to traditional technologies. However, in many experimental works, it has been demonstrated that the Coefficient Of Performance (COP) is very low such as cooling power and temperature difference [18]. In this perspective, the University of Naples Federico II, University of Genoa, and the National Research Council (CNR), intend to design and develop the first elastocaloric Italian prototype. Theoretical studies on elastocaloric cooling are promising but still at the initial level. To date, elastocaloric prototypes are less than ten units in the world [19-23]. The design and development process of this novel idea of prototype is presented in this work. Besides, it is discussed about the SMA wires arrangement and the fluid management in an efficient, continuously cooling device.

2. ELASTOCALORIC MATERIALS - SMA

Since the 1980s, especially in the biomedical sector, SMAs have been used due to their superior superelastic mechanical performance. In the work of Jani et al. [14], a summary of various applications of shape memory alloys is presented. A literature analysis has been carried out using SCOPUS with search keyword "SMA material" for related areas and is presented in Figure 3. Properties of SMAs greatly impact the elastocaloric cooling system and their comprehension is a requisite to design and develop an elastocaloric device. Kirsch et al. [22] defined five important criteria of an elastocaloric material: 1) large latent heat; 2) low mechanical work input; 3) high functional stability; 4) good structural stability; 5) transformation temperature slightly below application temperature. To date, a SMA materials that have all the five characteristics are not available. Recent studies focus on the development of new optimized pseudoelastic materials for elastocaloric cooling by improving the material composition (quantifying the SMA phase transition temperature) [24] to achieve a large elastocaloric effect (that means a high adiabatic temperature change), to improve material stability and response and to make easier the fabrication processes.

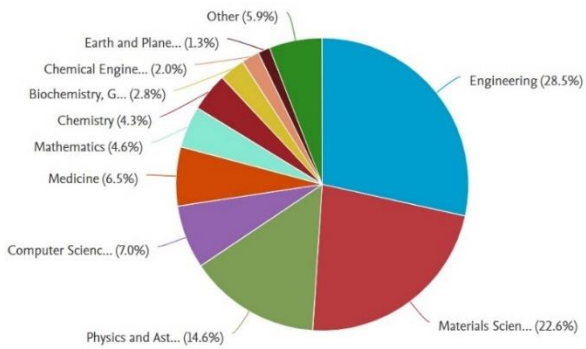

Figure 3. SMA publications from 1990 to 2021

As said in the previous paragraph, all SMAs can be considered potential elastocaloric materials if their

transformation temperatures (Af) are below the device's working temperature, which is a precondition for reversible superelasticity. It is possible to consider three different groups of the elastocaloric materials: shape memory alloy-based (NiTi-based, Cu-based, and Fe-based), shape memory polymer-based (SMP), and magnetic shape memory alloy-based (MSMA) as listed in work [25].

The elastoCaloric effect (eCe) can be defined as the temperature change (DT_{ad}) in the elastocaloric material following the application of the uniaxial stress in an adiabatic transformation. The material increases its temperature during loading and decreases it during unloading. If the process is isothermal, an entropy variation in the material itself is detected. These two quantities constitute a measure of the elastocaloric effect and they can be defined, respectively, by the following equations:

$$\Delta T_{ad} \approx -\frac{1}{\rho}\frac{T_0}{c}\Delta s_{iso} \tag{1}$$

$$\Delta s_{iso} \approx \frac{1}{\rho}\int_{\sigma_1}^{\sigma_2}\left(\frac{\partial \varepsilon}{\partial T}\right)_{\sigma} d\sigma \tag{2}$$

where, ρ is the material's density, ε the applied strain, σ the applied stress, c the material's specific heat, and T_0 the material's temperature. The equations above can be used only for estimating the adiabatic temperature changes if c is considered constant with temperature. A more precise and correct way of defining the adiabatic temperature changes is using the following equations [26]:

$$\Delta T_{ad} = T_2(S_{tot}, \sigma) - T_1(S_{tot}, \sigma = 0) \tag{3}$$

$$S_{tot} = S_{tot,\sigma=0} + \Delta s_{iso} \tag{4}$$

The total entropy at zero applied stress is defined as:

$$S_{tot,\sigma=0} = \int_{T_1}^{T_2}\frac{c}{T}dT \tag{5}$$

Usually, the specific heat c at zero stress (and at different temperatures) is obtained with calorimetry measurements.

The latent heat, ΔH, depends on the material's composition and microstructure of the work input [27]. A recent experimental approach to determine the latent heat is shown in Michaelis et al. [15]: a direct electrical power input replaces the latent heat of the elastocaloric material absorbed via adiabatic loading during the first strain loading pulse of the tensile cycle.

Many studies proposed NiTi-based as elastocaloric materials due to data on phase transformation temperatures and latent heats for ternary NiTi-based or quaternary NiTiCu-based SMAs. In the study [28], it has been demonstrated a strong dependence of transformation temperatures and latent heat on Ni concentration. Their study shows a correlation between transformation temperatures, A_f, and the latent heat ΔH, as shown in Figure 4.

It is evident a linear behaviour by adding Ni, Cr, Co, Fe, and V to stoichiometric NiTi: a decrease in A_f is always associated with a decrease in latent heat. In binary Ni-Ti shape memory alloys, the latent heats ΔH of the transformation from austenite to martensite decrease when Ni is added to stoichiometric NiTi; this decrease in ΔH directly results in a decrease of A_f. Figure 5 shows the latent heat of transformation from austenite to martensite as a function of the width of the thermal hysteresis ΔT.

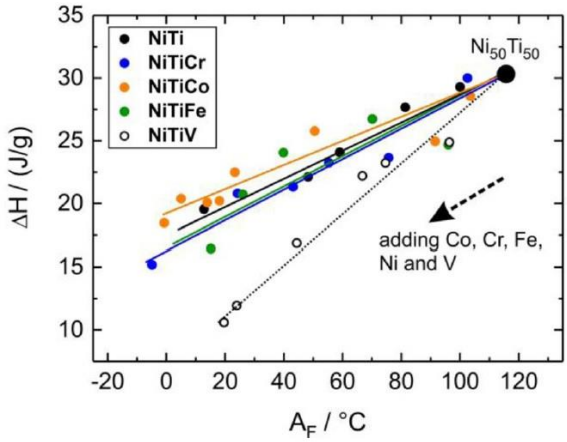

Figure 4. Latent heats ΔH and transformation temperatures correlation for various NiTi-based SMAs [20]

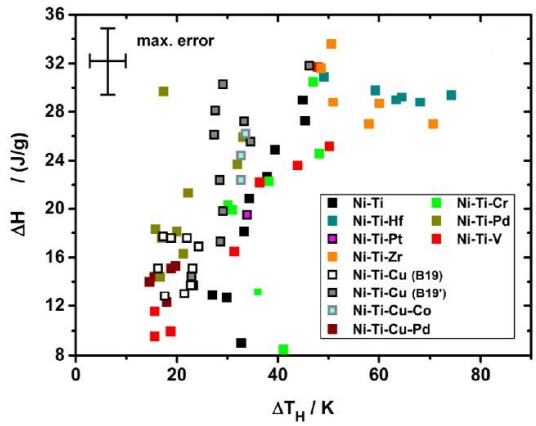

Figure 5. Key parameters: latent heat and width of thermal hysteresis

Low thermal hysteresis widths and large latent heat in the elastocaloric cooling are fundamental to choose the SMA materials to obtain a high cooling efficiency because thermal hysteresis is directly proportional to the mechanical hysteresis width, as demonstrated in the experimental analysis of Jaeger et al. [25]. From the literature, it is possible to determine a good compromise of SMA elastocaloric material with a high coefficient of performance (COP): the quaternary SMA NiTiCuV. The quaternary SMA NiTiCuV provides promising elastocaloric properties and shows minor functional effects during thermomechanical training.

The decrease in mechanical hysteresis and residual strain leads to a decrease in latent heat and transformation temperatures. In contrast, the mechanical and caloric parameters show a more significant change during the austenite to martensite transformation. The reverse transformation has resulted stable; this fact improves the performance of the cooling process [29].

3. ACTIVE CALORIC REGENERATIVE PROCESS

The active caloric regenerative process is more efficient than typical vapour compression; for this reason, many

research studies and comprehensive reviews on modelling and experiments can be found in the literature, especially for magnetocaloric refrigeration [17].

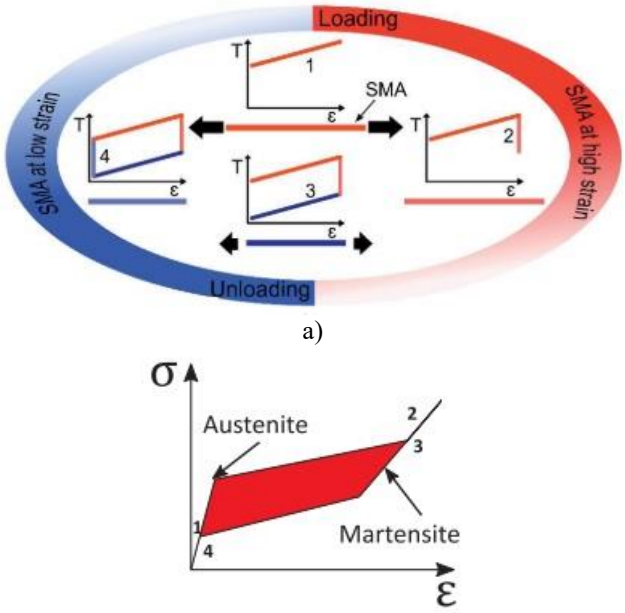

Figure 6. a) Trend of the SMA temperature as a function of strain ε in the four-stage cycle (adiabatic cooling cycle); b) Corresponding stress-strain

According to Figure 6a, four steps form an active regenerative thermodynamic cycle: the caloric Brayton-like active regenerative cycle. The four steps can be named: *loading, heat transfer (heating); unloading; heat transfer (cooling).*

Loading: during this process, mechanical loading is applied to the elastocaloric material in adiabatic conditions. Applied stress is enough to activate the transformation from austenite to martensite (elastocaloric). The temperature of caloric material increases up to a specific temperature (ΔT_{ad}).

Heat transfer (heating): the working fluid (typically air or water) flows through the caloric material. The temperature T_f (fluid temperature) increases, while the temperature caloric material decreases.

Unloading: the stress is reduced adiabatically, which means that the caloric material is exposed to an adverse change of the field. Consequently, it happens the transformation from martensite to austenite, decreasing the temperature of the caloric material.

Heat transfer (cooling): the working fluid flows through the caloric material and cools down. Therefore, the temperature T_f decreases while the temperature of the elastocaloric material increases. In this last step, the heat transfer fluid at a temperature lower than the room temperature can be used to subtract heat and realize the useful effect of the cycle.

3.1 Active elastocaloric regenerative process - AeR

Most of the work related to the elastocaloric effect is still based on the Nitinol alloy (NiTi).

The refrigerant SMA works between the ambient temperature T_{amb} and the cooling temperature T_c [30]. In the beginning, the material is in the austenite phase at zero stress condition. The transition from austenite to martensite phase occurs when sufficient driving stress is applied. The heat transfer between SMA and the working fluid takes place at constant high strain. The contact remains until thermal equilibrium is achieved. Later, adiabatic unloading decreases the SMA temperature below the temperature level of the heat source. This effect results from endothermic and adiabatic phase transformations from martensite to austenite. Finally, the cold SMA absorbs heat from the working fluid until the thermal equilibrium is reached. The entire cycle is shown in Figure 6a.

Figure 6b shows the work of an elastocaloric cycle. The area inside the hysteresis curve is the nonrecoverable work; besides being a small temperature range, the exponential curves appear linear. The isentropic phase transformations during adiabatic loading and unloading do not consider any irreversibilities.

3.1.1 Cooling efficiencies of elastocaloric cycles

In the work of Schmidt et al. [31], a graphical approach is proposed to determine the work and the absorbed heat of an elastocaloric cooling process. Their approach starts from an analytical description of the mechanical and thermal behavior (page 87 of [32]). Besides, they validated the graphical approach with an experimental approach.

The specific mechanical work (w) is determined by:

$$w = \frac{1}{\rho}\sigma\Delta\varepsilon \tag{6}$$

The specific mechanical work for the entire cycle (w_0) is equivalent to the integral over the four process steps of Figure 6b:

$$w_0 = \frac{1}{\rho}\oint \sigma \, d\varepsilon \tag{7}$$

By neglecting the irreversible contributions to the entropy change, the absorbed heat q_{ab} during the transition from phase four to phase one is derived from the following equation:

$$q_{ad} = \int T \, ds \tag{8}$$

The COP of the elastocaloric cooling cycle can be calculated as:

$$COP = \frac{q_{ad}}{w_0} \tag{9}$$

4. STATE-OF-ART ABOUT ELASTOCALORIC PROTOTYPES

This paragraph presents the elastocaloric cooling models of the various devices existing in the literature.

The most used alloy is the NiTi-based one as they have more developed shape memory properties, readily available on the market, and have an acceptable useful life for elastocaloric applications. Other elements can be added to these alloys to increase the latent heat and increase the transformation temperature and the alloy's useful life. It was shown in work [33] that NiTiCu alloys can provide 10 million cycles without breaking. Lately, Cu and Fe-based alloys are used in elastocaloric processes thanks to their lower cost and the possibility of having the elastocaloric effect with a lower stress

than the NiTi-based alloys. As far as copper-based alloys are concerned, they can generate remarkable performance coefficients thanks to the fact that they show a considerable variation in temperature [30]. Iron-based alloys have a much longer service life [31] than copper or NiTi-based alloys, but due to their lower latent heat, they cannot achieve acceptable results in elastocaloric terms. It has been shown that with a compressive stress of the NiTi alloy, it is possible to perform 10 000 cycles, while with similar tensile stress, the actual cycles are only 165, as shown in the work of Wu et al. [34]. Their work demonstrates that the application of effort is a determining factor in obtaining the elastocaloric effect in shape memory alloys, small hysteresis (thermal and mechanical) and durability.

Despite the progress made in searching for the best alloy to be used in elastocaloric devices, the latter is still in an experimental phase of optimization and therefore are not yet ready for commercialization. The devices presented to the scientific community, to date, are based on one-shot applications: the elastocaloric material is in contact, alternatively, with air (or water) while it is subjected to mechanical stress [22, 35]. In the works [22, 35] regenerative devices were presented: the elastocaloric material is formed by a series of wires or plates (or tubes) arranged radially with two co-rotating discs. The discs rotating continuously allow the wires to be stretched along the semicircle and rest along the other semicircle. This model allows having hot and cold air to flow at the same time.

Finally, currently, the way to transfer the uniaxial stress to the elastocaloric materials are those with mechanical or hydraulic pistons.

4.1 Suggestions on future developments of the elastocaloric cooling

As previously mentioned, the prototypes presented to the scientific community are still far from being commercialized on a large scale. In the last decade, efforts have intensified to create high-caloric refrigeration prototypes for the conditioning of residential environments. As Engelbrecht also suggests in his work [36], future devices must manage to improve the following points:

- increase the system temperature range from less than 20 ° C to at least 40°C;
- increase the fatigue life of eCMs in devices to over 1 million cycles;
- find a practical solution to apply stress;
- demonstrate high efficiency;
- increase cooling capacity to suit end-user applications;
- coupling of the elastocaloric cooler with external components such as heat exchangers and efficient fluid circulators;
- development of control schemes and cycle fine-tuning;
- design an economical and efficient system.

Increasing the system's temperature range is undoubtedly the most significant challenge since obtaining a device that can also be used for commercial applications would considerably reduce the environmental pollution that vapour compression refrigeration generates.

Techniques for fatigue enhancement of NiTi alloys were presented in the work of Tusek et al. [37]. The work demonstrates that by applying an initial pre-deformation (up to 10%) and performing an intermediate deformation cycle around the midpoint of the exhaust deformation plateau, significant results can be obtained to increase the fatigue life of the elasto-caloric material. The effect, therefore, leads to an increase in the number of cycles useful for elasto-caloric refrigeration.

A further way to improve the material's fatigue life is to limit the stress applied to the material; in fact, in the works presented, it has been shown to obtain the elastocaloric effect, in NiTi alloys, a stress of about 450 MPa and a deformation of about 3% is mandatory. The applied stress is very high; therefore, creating alloys with other elements would control the phenomenon of interstellation [33, 38] and reduce stress: the CuZnAl alloy requires stress of about 250 MPa [39]. Furthermore, in addition to compression and traction, in a recent study [37], it was shown that the application of torsion allows for a longer useful life and higher temperatures with significantly lower stresses. In fact, in their work, they state that a PVDF coil's coefficient of performance (polyvinylidene difluoride) for twist-calorie cooling has reached a value as high as 8.8.

Table 1 summarizes all the devices made to date presented by the scientific community.

When the above points are optimized, it will also be possible to determine a possible elasto-caloric device price. The key difference with vapour compression devices is that the elastocaloric devices work with low-pressure fluids. Therefore, the hydronic circuits used in the device are cheaper and lighter than a vapour compression device.

5. THE FIRST ITALIAN PROTOTYPE

This section intends to illustrate the design choices aimed at creating an elastocaloric prototype in continuous operation. Therefore, the choice falls on developing a rotary type prototype as it, unlike an alternating configuration, is to guarantee the objective above.

As shown in Figure 7a, by placing multiple strands of eCM on a concentric circumference to another (for example, the circumferences of two discs), the two discs' synchronous rotation allows the elements of eCM to experience different phases of the cycle at the same time.

During the rotation, some wires will be in traction. Others will be in the relaxation phase allowing a continuous flow of cold air because each wire will experience during one rotation one complete cycle. The cyclical traction (loading) and relaxation (unloading) of the eCM induce a temperature profile along the device's circumference. As already pointed out in the introduction of the AeR cycle, the heat exchanges between the eCM and the environments (hot and cold), thanks to an auxiliary fluid, occur through a convective heat exchange (fluid-solid).

In the first version, we intend to develop and implement the elastocaloric cooler prototype as a direct air cooling unit, avoiding additional heat exchangers. Although it has lower heat transfer characteristics than liquids (smaller values of convective conductance), air offers easier handling and a more straightforward mechanical design.

There are no problems with sealing and accidental leaks. The duct, or rather the confined space reserved for the passage of air, consists of two concentric cylinders. The air flows in the annular region along the longitudinal direction, thus meeting the strands of eCM, transversely, as shown in Figure 7b. An appropriate arrangement of the air inlets and outlets on each semicircle allows the continuous extraction of hot and

cold air. As shown in Figure 7b, the airflow orthogonally laps the threads of eCM while in counter-rotation concerning the fluid's motion. This design solution allows to facilitate the path of the air in the device and at the same time to operate at higher frequencies, with the consequent increase in cooling power (cooling thermal power).

Table 1. Elastocaloric cooling device to date

Type	Dimensions	Stress Type	Material*	Cycle	Fluid	COP	Year	Reference
SMA ribbon plate	Length = 90 mm Width = 3.2 mm Thickness = 0.5 mm	linear tensile – max load 750 MPa	$Ni_{50.8}Ti_{49.2}$	One shot	Air	N.A.	2015	[35]
SMA ribbon plate	Length = 15 mm Width = 1.75 mm Thickness = 0.02 mm	linear tensile – max load 520 MPa	$Ni_{50.4}Ti_{49.6}$ $Ni_{29.6}Ti_{55}Cu_{12.6}Co_{2.8}$	One shot	Air	2.9-3.1 2.9	2016	[40]
SMA foils	Length = 15 mm Width = 2 mm Thickness = 0.03 mm	deflection on the bridge center	$Ni_{50.5}Ti_{49.1}Fe_{0.4}$	Cascade	Air	3.2	2017	[41]
SMA film/foil	Length = 5-30 mm Width = 0.5-3 mm Thickness = 0.03 mm	deflection on the bridge center	$Ni_{30.7}Ti_{54.7}Cu_{12.3}Co_{2.3}$ NiTiFe	Cascade Cascade	Air Air	6.7 5.5	2018	[42]
SMA ribbon plate	Length = 50 mm Width = 10 mm Thickness = 0.2 - 0.3 mm	linear tensile	$Ni_{55.8}Ti_{44.2}$ $Ni_{56}Ti_{44}$	Regenerative Regenerative	Water Water	N.A. N.A.	2017	[43]
Wires	Length = 30 mm D_w = 0.2 mm	Rotary tensile	N.A.	Regenerative	Air	N.A.	2018	[44]
Fiber	Diameter = 0.33 mm	Twist	PVDF polymer	One shot	Air	8.8	2020	[45]

*percentage by weight

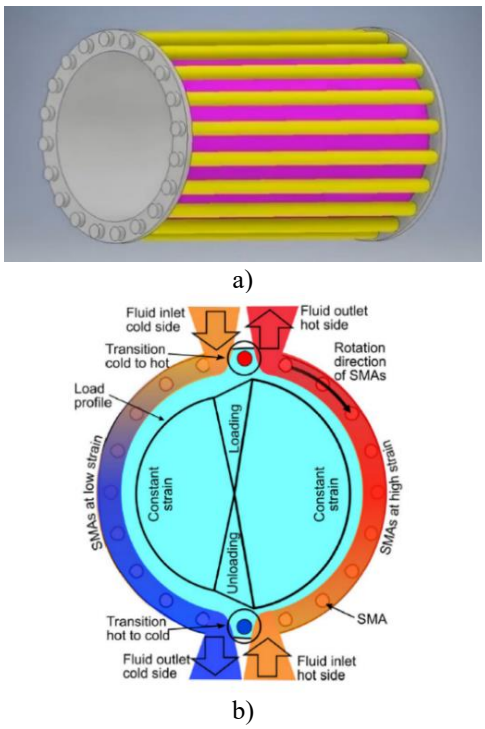

Figure 7. a) Sketch of the concept of the first Italian eC device; b) Heat transfer channel and direction of fluid flow

The latent heat released and absorbed by the eCM, along the two semi-circumferences during the loading and unloading phases, is exchanged with the air by heating and cooling it, respectively. Supposing that the prototype works with optimized operating conditions (speed and mass flow rate of the air, rotation frequency, intensity of the loading and unloading stress), it is possible to observe a hot and a cold semicircle, stationary, even if the fluid rotates. Therefore, adequate sizing and a suitable choice of operating conditions allow for continuous operation. It is also possible to concentrate many eCMs in a small space, thus optimizing the device's space and assembly.

The device has dimensions typical of macro-scales. It is designed for an environmental conditioning type application that can be an alternative to current systems on the market, based on conventional vapor compression technology. The eCM to be used as a refrigerant is a NiTi alloy. The appropriate composition will be studied in a preliminary phase of study and testing on materials conducted at the Heat Transfer Laboratory of the University of Naples Federico II.

What emerges from this description is the presence of many design parameters to be appropriately chosen. Besides, a study on the optimization of the material in terms of composition and shape is necessary.

5.1 Design and realization

As anticipated in the previous section, the dimensional target to which the prototype is built is macro-scale. It is designed for an environmental conditioning type application that can be an alternative to the current market systems based on conventional vapor compression technology.

We intend to build a prototype that globally occupies a cylindrical volume, 60-70 cm long and 30-35 cm in diameter for a total occupied volume of 0.042-0.067 m^3. The purpose is to maximize the cooling power; from the following relationship, it depends on the mass of the cooling material and the rotation frequency of the cylinder, as well as obviously on the latent heat of the material:

$$\dot{Q} = \frac{m}{t}\Delta H = mf\Delta H \quad (10)$$

ΔH is the latent heat of eCM (typically for NiTi array is equal to 11 J/g). It is possible to act on the rotation frequency and the quantity of eCM, to increase the prototype's cooling power.

The greater the amount of material used, the higher the observable cooling power will be. Therefore, it is necessary to find efficient design solutions to implement the prototype with a high mass of eCM in a small space (volume of the prototype).

To make an AeR cycle efficiently, the choice of the most appropriate frequency, it is necessary to highlight that the maximum admissible rotation frequency is equal to:

$$f = \frac{1}{2t_c} = \frac{1}{4\tau} \quad (11)$$

t_c is the time transfer of the fluid into the channel while τ is the thermal time constant. Since the Biot number is always lower than 0.1, it is always possible to neglect the temperature distribution of the wire, assuming an exponential temperature evolution. The time constant can be defined as:

$$\tau = \frac{\rho c}{4h} D_w \quad (12)$$

The relationships above suggest working with a high mass of eCM, consisting of small elements with small diameter:

$$m = n_w m_w \quad (13)$$

$$m_w = \rho_w V_w \quad (14)$$

It is, therefore, possible to implement the eCM as an array containing a large number of long filiform elements, in the absence of applied stress, 30-50 cm long and with a tiny diameter.

5.2 Some preliminary calculations

Supposing the NiTi wires with a length equal to 0.5 m and diameter values between 0.3 mm and 1 mm, the values of heat transfer coefficient *h*, *f*, and *Q,* varying the air flow velocity at fixed number of wires, have been calculated. The Nusselt number has been evaluated with the Whitaker [45-48] correlation:

$$Nu = \frac{h\,D_w}{k} = \left(0.40\,Re^{\frac{1}{2}} + 0.06\,Re^{\frac{2}{3}}\right) Pr^{2/5} \quad (15)$$

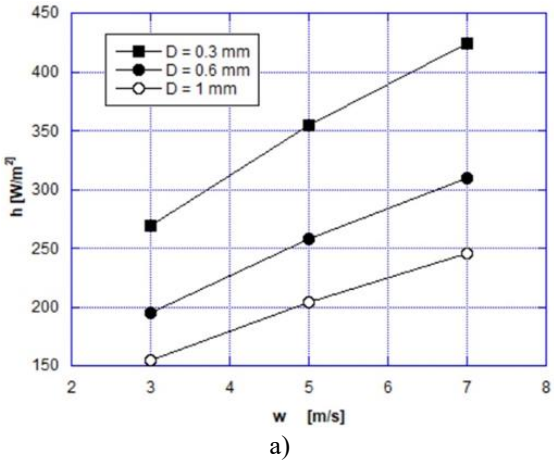

a)

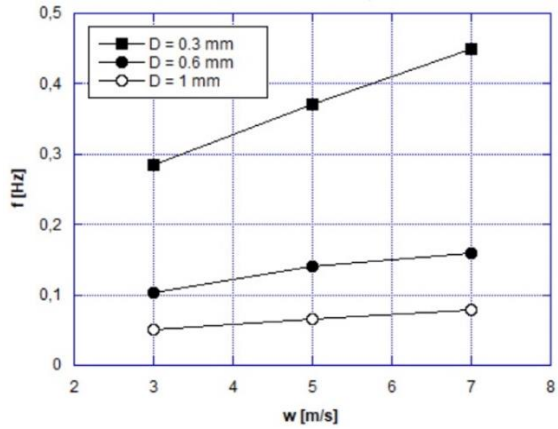

b)

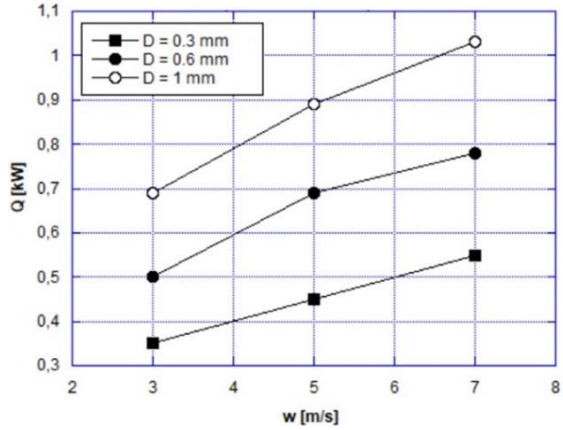

c)

Figure 8. Heat transfer coefficient (a), frequency (b), and the cooling power Q (c) as a function of air velocity and wire's diameter

In Figures 8 (a, b, c) is reported the heat transfer coefficient, the cycle frequency and the cooling power as a function of air velocity varying the wire diameter for a fixed number of wires (500). The reported results clearly show that increasing the air flow velocity at constant wire diameter, the heat transfer coefficient also increases with the cycle frequency and therefore the cooling power. Therefore, the higher is the air velocity the higher is the cooling power.

From figure 8 (c), it is clear that using wires with a diameter of 1 mm the cooling power is higher than with a smaller diameter. The result shown is for the same number of wires with different diameters. Therefore, this is due to the greater mass of SMA corresponding to a greater diameter. Indeed, decreasing the wire diameter the heat transfer coefficient decreases together with the cycle frequency. Nevertheless, the effect of the increase of SMA mass prevails.

In Figure 9 is reported the cooling power as a function of the wire diameter for three values of the air velocity (i.e. 3,5,7 m/s) at fixed SMA mass (111 g). At fixed SMA mass, the smaller is the wire diameter, the smaller the heat exchange time constant, the higher the maximum permissible rotation frequency and, consequently, the greater the cooling power. Furthermore, for diameters larger than 0.5 mm, a higher tension force is required, and this generates a more significant expenditure of mechanical energy, reducing the COP. The figure clearly shows also that at fixed diameter the cooling power increases with air velocity, but this trend is more marked at lower velocity values.

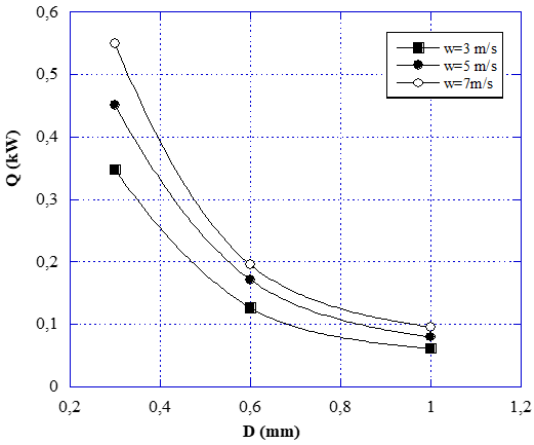

Figure 9. Cooling power as a function of the wire diameter varying the air velocity

6. CONCLUSIONS

In Europe, the residential sector has the highest energy consumption (about a quarter of the total) in refrigeration. Therefore, decreasing energy consumption in this sector is a primary objective. Many initiatives have arisen to develop renewable energy technologies in this sector as well. However, these new technologies are characterized by high installation costs and extremely long payback times.

In this work, a new way of refrigerating is illustrated: elastocaloric refrigeration. A prior art eC system shows promising performance in terms of generated temperature spam, cooling/heating capacity, and COP. The fatigue life of eCMs is a problematic issue in the commercialization of eC devices. This problem can be addressed by designing new material systems, using new manufacturing methods, and developing new devices.

It is presented the preliminary steps to design and develop the first Italian eC device. The choice falls on the development of a prototype in a rotating configuration. Applying NiTi wires as SMA, into the prototype, initial calculations are made. The first results highlighted the importance of using thin wires (<0.5 mm in diameter) to obtain high frequencies and, consequently, a high cooling power value. Furthermore, the direct proportionality of the eCM mass with the cooling power requires us to install a large number of wires inside our prototype.

ACKNOWLEDGMENT

This research was funded through the project “SUSSTAINEBLE" - FISR2019 04798 granted by FISR – Fondo Integrativo Speciale per la Ricerca (Italian special supplementary fund for research).

REFERENCES

[1] Manca, O., Cirillo, L., Nardini, S., Buonomo, B., Ercole, D. (2016). Experimental investigation on fluid dynamic and thermal behavior in confined impinging round jets in aluminum foam. Energy Procedia, 101: 1095-1102. https://doi.org/10.1016/j.egypro.2016.11.149

[2] Buonomo, B., Cirillo, L., Manca, O., Mansi, N., Nardini, S. (2016). Confined impinging jets in porous media. In Journal of Physics: Conference Series, 745(3): 032142. https://doi.org/10.1088/1742-6596/745/3/032142

[3] Protocol, M. (1987). On Substances that Deplete the Ozone Layer. Vienna.

[4] Greco, A., Mastrullo, R., Palombo, A. (1997). R407C as an alternative to R22 in vapour compression plant: An experimental study. International Journal of Energy Research, 21(12): 1087-1098. https://doi.org/10.1002/(SICI)1099-114X(19971010)21:12<1087::AID-ER330>3.0.CO;2-Y

[5] Greco, A., Vanoli, G.P. (2006). Experimental two-phase pressure gradients during evaporation of pure and mixed refrigerants in a smooth horizontal tube. Comparison with correlations. Heat and Mass Transfer, 42(8): 709-725. https://doi.org/10.1007/s00231-005-0020-7

[6] Greco, A., Vanoli, G.P. (2005). Flow boiling heat transfer with HFC mixtures in a smooth horizontal tube. Part II: Assessment of predictive methods. Experimental Thermal and Fluid Science, 29(2): 199-208. https://doi.org/10.1016/j.expthermflusci.2004.03.004

[7] Aprea, C., Greco, A., Maiorino, A., Masselli, C. (2018). The drop-in of HFC134a with HFO1234ze in a household refrigerator. International Journal of Thermal Sciences, 127: 117-125. https://doi.org/10.1016/j.ijthermalsci.2018.01.026

[8] Aprea, C., Greco, A., Maiorino, A. (2017). An experimental investigation of the energetic performances of HFO1234yf and its binary mixtures with HFC134a in a household refrigerator. International Journal of Refrigeration, 76: 109-117. https://doi.org/10.1016/j.ijrefrig.2017.02.005

[9] Greco, A., Aprea, C., Maiorino, A., Masselli, C. (2019). A review of the state of the art of solid-state caloric cooling processes at room-temperature before 2019. International Journal of Refrigeration, 106: 66-88. https://doi.org/10.1016/j.ijrefrig.2019.06.034

[10] Goetzler, W., Zogg, R., Young, J., Johnson, C. (2014). Alternatives to vapor-compression HVAC technology. ASHRAE Journal, 56(10): 12.

[11] Pecharsky, V.K., Gschneidner Jr, K.A. (1999). Magnetocaloric effect and magnetic refrigeration. Journal of Magnetism and Magnetic Materials, 200(1-3): 44-56. https://doi.org/10.1016/S0304-8853(99)00397-2

[12] Aprea, C., Greco, A., Maiorino, A., Masselli, C. (2020). The use of barocaloric effect for energy saving in a domestic refrigerator with ethylene-glycol based nanofluids: A numerical analysis and a comparison with a vapor compression cooler. Energy, 190: 116404. https://doi.org/10.1016/j.energy.2019.116404

[13] Cui, J., Wu, Y., Muehlbauer, J., Hwang, Y., Radermacher, R., Fackler, S. (2012). Demonstration of high efficiency elastocaloric cooling with large ΔT using NiTi wires. Applied Physics Letters, 101(7): 073904. https://doi.org/10.1063/1.4746257

[14] Jani, J.M., Leary, M., Subic, A., Gibson, M.A. (2014). A review of shape memory alloy research, applications and opportunities. Materials & Design (1980-2015), 56: 1078-1113. https://doi.org/10.1016/j.matdes.2013.11.084

[15] Michaelis, N., Welsch, F., Kirsch, S.M., Schmidt, M., Seelecke, S., Schütze, A. (2019). Experimental parameter identification for elastocaloric air cooling. International Journal of Refrigeration, 100: 167-174.

https://doi.org/10.1016/j.ijrefrig.2019.01.006
[16] Kitanovski, A., Plaznik, U., Tomc, U., Poredoš, A. (2015). Present and future caloric refrigeration and heat-pump technologies. International Journal of Refrigeration, 57: 288-298. https://doi.org/10.1016/j.ijrefrig.2015.06.008
[17] Aprea, C., Greco, A., Maiorino, A., & Masselli, C. (2020). The employment of caloric-effect materials for solid-state heat pumping. International Journal of Refrigeration, 109: 1-11. https://doi.org/10.1016/j.ijrefrig.2019.09.011
[18] Aprea, C., Greco, A., Maiorino, A., Masselli, C. (2017). Analyzing the energetic performances of AMR regenerator working with different magnetocaloric materials: Investigations and viewpoints. Int. J. Heat Technol, 35: S383-S390. https://doi.org/10.18280/ijht.35Sp0152
[19] Michaelis, N., Welsch, F., Kirsch, S.M., Schmidt, M., Seelecke, S., Schütze, A. (2018). Investigation of single wire elastocaloric air cooling potential. In Thermag VIII, pp. 167-172.
[20] Kirsch, S.M., Welsch, F., Michaelis, N., Schmidt, M., Wieczorek, A., Frenzel, J. (2018). NiTi ‐ Based Elastocaloric Cooling on the Macroscale: From Basic Concepts to Realization. Energy Technology, 6(8): 1567-1587. https://doi.org/10.1002/ente.201800152
[21] Welsch, F., Kirsch, S.M., Michaelis, N., Motzki, P., Schütze, A., Seelecke, S. (2019). Continuous operating elastocaloric heating and cooling device: model-based parameter study with airflow losses. In Smart Materials, Adaptive Structures and Intelligent Systems, 59131: V001T04A020. https://doi.org/10.1115/SMASIS2019-5636
[22] Kirsch, S.M., Welsch, F., Michaelis, N., Schmidt, M., Wieczorek, A., Frenzel, J. (2018). NiTi-based Elastocaloric cooling on the macroscale: From basic concepts to realization. Energy Technology, 6(8): 1567-1587. https://doi.org/10.1002/ente.201800152
[23] Tušek, J., Engelbrecht, K., Pryds, N. (2016). Elastocaloric effect of a Ni-Ti plate to be applied in a regenerator-based cooling device. Science and Technology for the Built Environment, 22(5): 489-499. https://doi.org/10.1080/23744731.2016.1176809
[24] Chen, Z., Cong, D., Li, S., Zhang, Y., Li, S., Cao, Y. (2021). External-field-induced phase transformation and associated properties in a Ni50Mn34Fe3In13 metamagnetic shape memory wire. Metals, 11(2): 309. https://doi.org/10.3390/met11020309
[25] Kabirifar, P., Žerovnik, A., Ahčin, Ž., Porenta, L., Brojan, M., Tušek, J. (2019). Elastocaloric cooling: state-of-the-art and future challenges in designing regenerative Elastocaloric devices. Strojniski Vestnik/Journal of Mechanical Engineering, 65. https://doi.org/10.5545/sv-jme.2019.6369
[26] Tušek, J., Engelbrecht, K., Mañosa, L., Vives, E., Pryds, N. (2016). Understanding the thermodynamic properties of the elastocaloric effect through experimentation and modelling. Shape Memory and Superelasticity, 2(4): 317-329. https://doi.org/10.1007/s40830-016-0094-8
[27] Frenzel, J., Eggeler, G., Quandt, E., Seelecke, S., Kohl, M. (2018). High-performance elastocaloric materials for the engineering of bulk-and micro-cooling devices. MRS Bulletin, 43(4): 280-284. https://doi.org/10.1557/mrs.2018.67
[28] Frenzel, J., Wieczorek, A., Opahle, I., Maaß, B., Drautz, R., Eggeler, G. (2015). On the effect of alloy composition on martensite start temperatures and latent heats in Ni–Ti-based shape memory alloys. Acta Materialia, 90: 213-231. https://doi.org/10.1016/j.actamat.2015.02.029
[29] Jaeger, S., Maaß, B., Frenzel, J., Schmidt, M., Ullrich, J., Seelecke, S. (2015). On the widths of the hysteresis of mechanically and thermally induced martensitic transformations in Ni–Ti-based shape memory alloys. International Journal of Materials Research, 106(10): 1029-1039. https://doi.org/10.3139/146.111284
[30] Tan, J., Wang, Y., Xu, S., Liu, H., Qian, S. (2020). Thermodynamic cycle analysis of heat driven elastocaloric cooling system. Energy, 197: 117261. https://doi.org/10.1016/j.energy.2020.117261
[31] Schmidt, M., Kirsch, S. M., Seelecke, S., Schütze, A. (2016). Elastocaloric cooling: from fundamental thermodynamics to solid state air conditioning. Science and Technology for the Built Environment, 22(5): 475-488. https://doi.org/10.1080/23744731.2016.1186423
[32] Brokate, M., Kenmochi, N., Müller, I., Rodriguez, J.F., Verdi, C. (1993). Phase transitions and hysteresis (Montecatini Terme). Lecture Notes in Mathematics.
[33] Chluba, C., Ge, W., de Miranda, R.L., Strobel, J., Kienle, L., Quandt, E., Wuttig, M. (2015). Ultralow-fatigue shape memory alloy films. Science, 348(6238): 1004-1007. https://doi.org/10.1126/science.1261164
[34] Wu, Y., Ertekin, E., Sehitoglu, H. (2017). Elastocaloric cooling capacity of shape memory alloys–Role of deformation temperatures, mechanical cycling, stress hysteresis and inhomogeneity of transformation. Acta Materialia, 135: 158-176. https://doi.org/10.1016/j.actamat.2017.06.012
[35] Schmidt, M., Schütze, A., Seelecke, S. (2015). Scientific test setup for investigation of shape memory alloy based elastocaloric cooling processes. International Journal of Refrigeration, 54: 88-97. https://doi.org/10.1016/j.ijrefrig.2015.03.001
[36] Engelbrecht, K. (2019). Future prospects for elastocaloric devices. Journal of Physics: Energy, 1(2): 021001. https://doi.org/10.1088/2515-7655/ab1573
[37] Tušek, J., Žerovnik, A., Čebron, M., Brojan, M., Žužek, B., Engelbrecht, K., Cadelli, A. (2018). Elastocaloric effect vs fatigue life: Exploring the durability limits of Ni-Ti plates under pre-strain conditions for elastocaloric cooling. Acta Materialia, 150: 295-307. https://doi.org/10.1016/j.actamat.2018.03.032
[38] Lu, B., Liu, J. (2017). Elastocaloric effect and superelastic stability in Ni–Mn–In–Co polycrystalline Heusler alloys: Hysteresis and strain-rate effects. Scientific Reports, 7(1): 1-11. https://doi.org/10.1038/s41598-017-02300-3
[39] Mañosa, L., Jarque-Farnos, S., Vives, E., Planes, A. (2013). Large temperature span and giant refrigerant capacity in elastocaloric Cu-Zn-Al shape memory alloys. Applied Physics Letters, 103(21): 211904. ttps://doi.org/10.1063/1.4832339
[40] Ossmer, H., Chluba, C., Kauffmann-Weiss, S., Quandt, E., Kohl, M. (2016). TiNi-based films for elastocaloric microcooling—fatigue life and device performance. APL Materials, 4(6): 064102. https://doi.org/10.1063/1.4948271
[41] Bruederlin, F., Ossmer, H., Wendler, F., Miyazaki, S., Kohl, M. (2017). SMA foil-based elastocaloric cooling:

from material behavior to device engineering. Journal of Physics D: Applied Physics, 50(42): 424003. https://doi.org/10.1088/1361-6463/aa87a2

[42] Bruederlin, F., Bumke, L., Chluba, C., Ossmer, H., Quandt, E., Kohl, M. (2018). Elastocaloric cooling on the miniature scale: A review on materials and device engineering. Energy Technology, 6(8): 1588-1604. https://doi.org/10.1002/ente.201800137

[43] Engelbrecht, K., Tušek, J., Eriksen, D., Lei, T., Lee, C. Y., Tušek, J., Pryds, N. (2017). A regenerative elastocaloric device: experimental results. Journal of Physics D: Applied Physics, 50(42): 424006. https://doi.org/10.1088/1361-6463/aa8656

[44] Wang, R., Zhou, X., Wang, W., Liu, Z. (2021). Twist-based cooling of polyvinylidene difluoride for mechanothermochromic fibers. Chemical Engineering Journal, 417: 128060. https://doi.org/10.1016/j.cej.2020.128060

[45] Whitaker, S. (1972). Forced convection heat transfer correlations for flow in pipes, past flat plates, single cylinders, single spheres, and for flow in packed beds and tube bundles. AIChE Journal, 18(2): 361-371. https://doi.org/10.1002/aic.690180219

[46] Qian, S., Geng, Y., Wang, Y., Muehlbauer, J., Ling, J., Hwang, Y. (2016). Design of a hydraulically driven compressive elastocaloric cooling system. Science and Technology for the Built Environment, 22(5): 500-506. https://doi.org/10.1080/23744731.2016.1171630

[47] Tušek, J., Engelbrecht, K., Eriksen, D., Dall'Olio, S., Tušek, J., Pryds, N. (2016). A regenerative elastocaloric heat pump. Nature Energy, 1(10): 1-6. https://doi.org/10.1038/nenergy.2016.134

[48] Qian, S., Geng, Y., Wang, Y., Ling, J., Hwang, Y., Radermacher, R. (2016). A review of elastocaloric cooling: Materials, cycles and system integrations. International Journal of Refrigeration, 64: 1-19. https://doi.org/10.1016/j.ijrefrig.2015.12.001

NOMENCLATURE

c	Specific Heat	J/kg K
COP	Coefficient of Performance	-
D	Diameter	mm
f	Frequency	Hz (s^{-1})
H	Latent Heat	J/g
h	Heat Transfer Coefficient	$W/m^2 K$
m	Mass	g
s	Entropy	J
T	Temperature	K
t_c	Transfer Time	s
V	Volume	m^3
w	Mechanical Work	J

Greek symbols

Δ	Differential	-
ε	Strain	-
σ	Stress	MPa
ρ	Density	kg/m^3
τ	Constant Time	s

Subscripts

ad	adiabatic
iso	isothermal
tot	total
w	wire